Hierarchical Self-Assembly of Amphiphilic Semiconducting Polymers into Isolated, Bundled, and Branched Nanofibers

Amanda C. Kamps, Michael Fryd, and So-Jung Park*

Department of Chemistry, University of Pennsylvania, Philadelphia, Pennsylvania 19104, United States

ABSTRACT

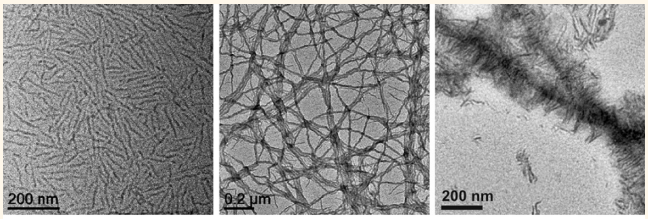

Herein, we report a high-yield click synthesis and self-assembly of conjugated amphiphilic block copolymers of polythiophene (PHT) and polyethylene glycol (PEG) and their superstructures. A series of different length PHT$_m$-*b*-PEG$_n$ with well-defined relative block lengths was synthesized by a click-coupling reaction and self-assembled into uniform and stably suspended nanofibers in selective solvents. The length of nanofibers was controllable by varying the relative block lengths while keeping other dimensions and optical properties unaffected for a broad range of f_{PHT} (0.41 to 0.82), which indicates that the packing of PHT dominates the self-assembly of PHT$_m$-*b*-PEG$_n$. Furthermore, superstructures of bundled and branched nanofibers were fabricated through the self-assembly of PHT$_m$-*b*-PEG$_n$ and preformed PHT nanofibers. The shape, length, and density of the hierarchical assembly structures can be controlled by varying the solvent quality, polymer lengths, and block copolymer/homopolymer ratio. This work demonstrates that complex superstructures of organic semiconductors can be fabricated through the bottom-up approach using preformed nanofibers as building blocks.

KEYWORDS: self-assembly · conjugated block copolymer · rod–coil · supramolecular nanostructures

Conjugated polymers have received a great deal of attention in recent years as an alternative to inorganic single-crystalline semiconductors due to their excellent optoelectronic properties and solution processability.[1−3] Among various conjugated polymers, poly(3-hexylthiophene) (PHT) has been one of the most widely studied semiconducting polymers in photovoltaic devices and field-effect transistors owing to its high hole mobility.[4,5] Unlike single-crystalline semiconductors, however, thin films of conjugated polymers possess many defects and impurities, and the device performance depends highly on the molecular packing of the polymers and on the nanometer scale film morphology.[6] In fact, the high mobility of PHT originates partly from its tendency to form well-packed crystalline domains.[7] However, typical thin films of conjugated polymers including PHT contain many grain boundaries and defects, which impede efficient charge transport.[8,9] Thus, the ability to control the polymer morphology is of paramount importance to fully exploit the potential of conjugated polymers in low-cost, flexible device fabrication.[10]

For the past two decades, there have been numerous studies aimed at optimizing the polymer morphology by employing various thin film processing techniques such as thermal or solvent vapor annealing.[11−13] Thin film self-assembly of conjugated block copolymers has recently emerged as a way to form ordered nanoarrays of conjugated polymers through the microphase segregation.[14−16] Solution-phase self-assembly of conjugated amphiphilic polymers offers a powerful alternative to the thin film techniques.[17−21] In this approach, conjugated polymers are organized into technologically relevant building blocks such as nanowires *via* the nature of amphiphilic polymers to self-assemble into various nanostructures. However, solution-phase self-assembly of conjugated amphiphilic polymers is not yet well understood, and the supramolecular self-assembly of such preformed building blocks into extended arrays by the bottom-up approach remains largely unexplored.

* Address correspondence to sojungp@sas.upenn.edu.

Received for review January 26, 2012 and accepted March 1, 2012.

Published online March 01, 2012
10.1021/nn300385p

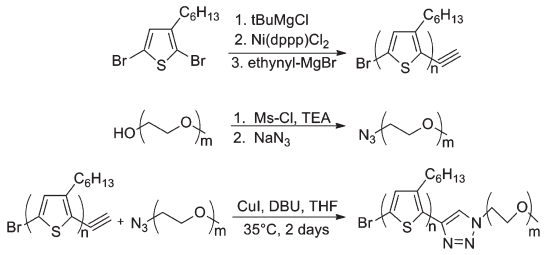

Scheme 1. Synthetic scheme for the click chemistry of PHT-*b*-PEG.

Here, we report the high-yield click-coupling synthesis and self-assembly of conjugated amphiphilic block copolymers composed of PHT and poly(ethylene glycol) (PEG) and their superstructures with preformed PHT nanofibers. The PEG block was chosen for its solubility in various solvents ranging from polar organic solvents to water, which makes it an excellent system for studying solution-phase self-assembly. A series of different length PHT-*b*-PEG copolymers were synthesized with precisely controlled molecular weights *via* the copper-catalyzed click reaction,[22] which enabled an accurate determination of the block lengths and the systematic correlation of the block ratio and the self-assembly structure. We show that PHT-*b*-PEG self-assembles into well-defined nanofibers with controllable lengths for a broad range of PHT weight fractions (f_{PHT}). Furthermore, we demonstrate that the self-assembly of PHT-*b*-PEG and preformed PHT nanofibers can lead to interesting superstructures such as closely packed nanofiber bundles and branched structures. The supramolecular self-assembly of PHT nanofibers presented here provides a new toolbox for the formation of novel organic nanostructures.

RESULTS AND DISCUSSION

Syntheses of PHT-*b*-PEG. A series of different length PHT-*b*-PEG copolymers were synthesized *via* the copper(I)-catalyzed click-coupling reaction of monoazide -terminated PEG (azide-PEG) and monoethynyl-terminated PHT (ethynyl-PHT) (Scheme 1). Ethynyl-PHT was synthesized using the living Grignard metathesis (GRIM) polymerization and the end functionalizaton method following a previously published procedure developed by McCullough.[23,24] The regioregularity (>95% HT) and the monoethynyl end group functionality of ethynyl-PHT were confirmed by ^{1}H NMR spectroscopy (Figure S1 in Supporting Information). The molecular weight and polydispersity of the ethynyl-PHT were determined to be 3428 g/mol and 1.16, respectively, by MALDI (Figure S2). The presence of the monoethynyl end group was also confirmed by MALDI-TOF (Figure S2). Azide-PEG was synthesized by the mesylation of the hydroxyl terminus of commercial methoxy PEG followed by sodium azide substitution (Scheme 1).[25,26] The presence of the azide end group was confirmed by FTIR spectroscopy (appearance of azide peak at 2101 cm^{-1}) (Figure S3) and by the end group analysis of MALDI spectra (Figure S4). A series of different length methoxy-PEGs were purchased and used to synthesize PHT-*b*-PEG with varying f_{PHT}. The molecular weight and PDI of azide-PEG were determined by MALDI and are presented in Table 1.

The synthesized ethynyl-PHT was coupled with a series of different length azide-PEG by the copper(I)-catalyzed azide−alkyne cycloaddition click reaction as described in Scheme 1 to generate PHT_{20}-*b*-PEG_n (n = 16, 48, 108) (Table 1). To avoid ethynyl homocoupling,[27] end-functionalized homopolymers were kept under inert conditions and used right after the synthesis (less than ~1 week). The chemical structure of the synthesized PHT-*b*-PEG was confirmed by ^{1}H NMR (Figure S5). The GPC data show that the retention time decreases with increasing molecular weight of PEG, confirming that the ethynyl-PHT and the azide-PEG are indeed coupled to yield PHT-*b*-PEG (Figure S6). The reaction yields were calculated to be over 70% for all synthesized polymers regardless of the PEG length (Table 1). This result contradicts the previous observation that a spacer between the ethynyl group and thiophene was necessary to avoid steric hindrance from the bulky alkyl side chains of PHT for the click syntheses of PHT-*b*-poly(styrene).[28]

Molecular weights of PHT-*b*-PEG were obtained by combining the predetermined molecular weights of PEG and PHT homopolymers (Table 1). An important advantage of the click chemistry of PHT-*b*-PEG is that the relative block lengths can be readily controlled by the choice of parent homopolymers. In contrast, in macroinitiation methods where the second polymer block is grown off of the end-functionalized conjugated polymer,[29,30] it can be challenging to precisely

TABLE 1. Molecular Weights and Molecular Weight Distributions of Synthesized PHT-*b*-PEG and Parent PHT and PEG Homopolymers

polymer	$M_{n,MALDI,PHT}$[a] (g mol^{-1})	$M_{n,MALDI,PEG}$[a] (g mol^{-1})	$M_w/M_{n,MALDI}$[a]	$M_{n,MALDI,PHT\text{-}b\text{-}PEG}$[b] (g mol^{-1})	$M_{n,GPC}$[c] (g/mol^{-1})	$M_w/M_{n,GPC}$[c]	f_{PHT}[a]
PHT_{20}	3428		1.16		6562	1.17	1.00
PHT_{20}-*b*-PEG_{16}	3428	761	1.04	4189	8489	1.21	0.82
PHT_{20}-*b*-PEG_{48}	3428	2169	1.05	5597	11710	1.22	0.61
PHT_{20}-*b*-PEG_{108}	3428	4896	1.04	8324	18200	1.21	0.41

[a] M_n, M_w/M_n, and f_{PHT} were determined by MALDI-TOF analysis. [b] M_n was determined by taking the sum of the homopolymer molecular weights as determined by MALDI-TOF analysis. [c] M_n and M_w/M_n were determined by GPC and are reported as their polystyrene equivalents.

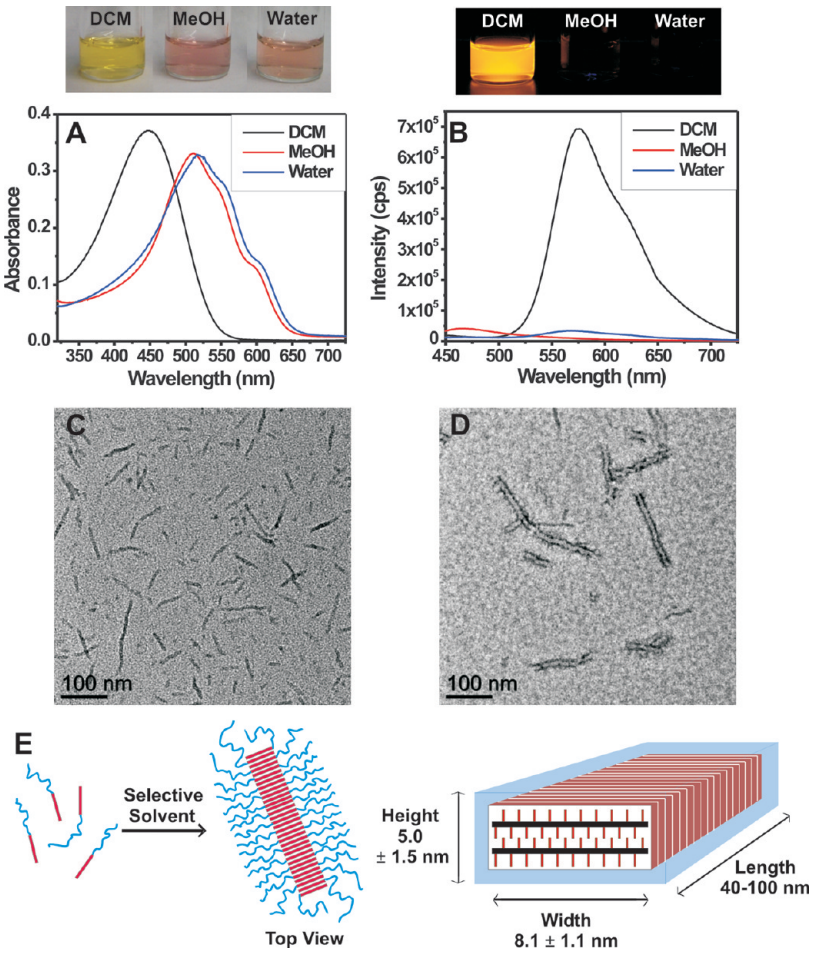

Figure 1. (A) Absorbance and (B) PL spectra of PHT_{20}-*b*-PEG_{108} dissolved in dichloromethane, methanol, and water at a concentration of 0.1 mg/mL. Pictures of PHT_{20}-*b*-PEG_{108} (0.1 mg/mL) solutions under ambient light (top-left) and under UV light (top-right) are given above the spectra. PL spectra were collected using an excitation wavelength of 380 nm. (C) TEM image of PHT_{20}-*b*-PEG_{108} assemblies formed in water. (D) TEM image of PHT_{20}-*b*-PEG_{108} assemblies stained with phosphotungstic acid solution, which visualizes PEG domains. (E) Schematic depiction of the nanofiber morphology formed from the self-assembly of amphiphilic PHT_{20}-*b*-PEG_{108} in a selective solvent.

control and characterize the polymer length.[31] Furthermore, due to the rigid nature of conjugated polymers, it is difficult to accurately determine the molecular weight of conjugated block copolymers by common techniques such as gel permeation chromatography (GPC).[32] In our synthesis of PHT-*b*-PEG, both PHT and PEG parent homopolymers were fully characterized by GPC, FTIR, NMR, and MALDI prior to the coupling reaction, which allowed for an accurate determination of the molecular weights of the resultant block copolymers and straightforward control of relative block lengths. As presented in Table 1, f_{PHT} was varied from 0.41 to 0.82 by changing the molecular weight of the PEG block while keeping the length of PHT constant. For comparison, molecular weights estimated using GPC with polystyrene standards are also given in Table 1. Note that many previous works on conjugated block copolymers reported the molecular weights determined by GPC despite the common knowledge that GPC overestimates the MW of rod-like polymers. The two sets of molecular weights presented in Table 1 clearly show that GPC significantly overestimates the molecular weights of PHT-*b*-PEG even for the polymers with small f_{PHT}, demonstrating an important advantage of click syntheses.

Self-Assembly in Selective Solvents. Due to its amphiphilic nature, PHT-*b*-PEG can be dispersed in a wide range of solvents. In polar organic solvents such as tetrahydrofuran (THF) and dichloromethane (DCM) where both polymer blocks are soluble, PHT-*b*-PEG exists as isolated chains and shows UV–vis and photoluminescence (PL) spectra that are characteristic of PHT homopolymers in good solvents (Figure 1A,B); the π–π^* absorption peak at ~450 nm and a high intensity PL at ~576 nm observed for PHT-*b*-PEG in DCM are characteristic of regioregular PHT in the same solvent.[33] This result indicates that the attachment of PEG does not significantly affect the conformation of PHT in good solvents. When PHT_{20}-*b*-PEG_{108} is dispersed in a selective solvent for PEG, such as water and methanol, the block copolymer organizes into supermolecular assemblies as evidenced by the red

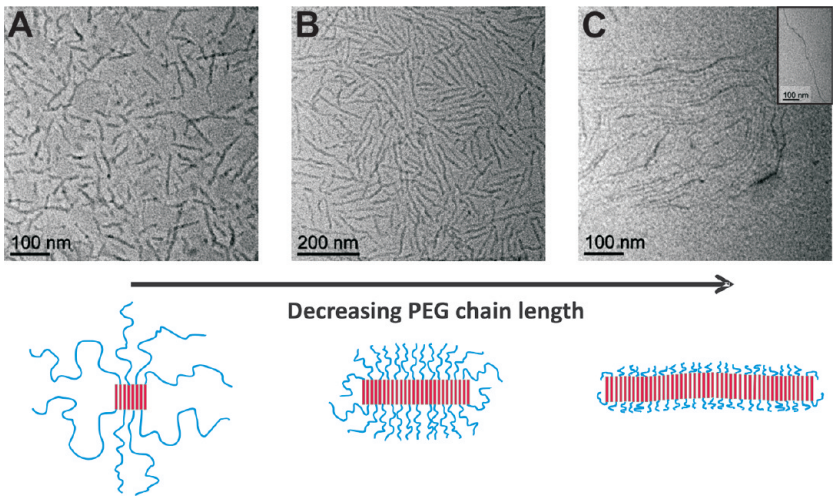

Figure 2. TEM images of PHT_{20}-*b*-PEG_n (n = 108, 48, 16) in water with varying f_{PHT}; (A) f_{PHT} = 0.41, (B) f_{PHT} = 0.61, and (C) f_{PHT} = 0.82. Below the respective TEM images is a schematic depiction of the effect of relative block lengths on the self-assembly structure.

shift and the appearance of the vibronic structure in the UV–vis spectra (Figure 1A); the red-shifted absorption peak is a result of the increased planarity of the packed PHT chains in polymer assemblies. The efficient PL quenching of PHT_{20}-*b*-PEG_{108} in selective solvents is also indicative of tightly packed PHT and strong interchain coupling in the polymer assemblies (Figure 1B).[17,34] Homopolymers of PHT also show a similar red shift and PL quenching upon the introduction of methanol (Figure S8). However, unlike PHT-*b*-PEG, PHT homopolymers form macroscopic aggregates and precipitate out of solution when the percentage of methanol was increased above 50%, which confirms that the covalently attached PEG block of the conjugated block copolymer is necessary to form stable suspensions of PHT assemblies.

The transmission electron microscopy (TEM) images in Figure 1C,D show that PHT_{20}-*b*-PEG_{108} self-assembles into one-dimensional fiber-like structures in selective solvents, with the darker contrast arising from the electron-dense PHT block. The PEG block was selectively stained with a phosphotungstic acid solution in Figure 1D, revealing the hydrophilic PEG block surrounding the PHT nanofiber core. The width of the PHT domain was measured to be 8.1 ± 1.1 nm, which corresponds to the length of one PHT_{20} chain calculated with the monomer length of 0.4 nm.[34] This indicates that the nanofiber is composed of interdigitated PHT chains surrounded by hydrophilic PEG chains, as depicted in Figure 1E. The height of the nanofibers was determined to be 5 ± 1.5 nm by AFM, while a lattice dimension of a PHT crystal unit cell corresponding to vertical stacks was reported to be 1.68 nm.[35–37] These data indicate that the PHT-*b*-PEG nanofibers are composed of 1–3 vertical stacks of PHT-*b*-PEG. These one-dimensional wire-like assemblies of semiconducting polymers are highly desirable for device applications as they can support high carrier mobility.[36] While the insulating block of semiconducting–insulating block copolymers can reduce the overall device performance, this effect can be overcome with highly ordered self-assembled systems.[38–40]

Effect of Relative Block Lengths on the Self-Assembly Structure of PHT-*b*-PEG. In order to examine the effect of block lengths on the self-assembly of PHT-*b*-PEG, the molecular weight of the PEG block was varied from 761 to 4896 g/mol while keeping the length of PHT constant, which yielded block copolymers with f_{PHT} = 0.41, 0.61, and 0.82 (Table 1). For all polymers examined in this study, PHT-*b*-PEG self-assembled into the same morphology of nanofibers in selective solvents (Figure 2). In general, coil–coil block copolymers self-assemble into various assembly structures such as simple micelles, cylindrical micelles, and vesicles depending on the relative block lengths and the Flory–Huggins parameters of the two polymers.[41] Rod–coil block copolymers have additional factors contributing to the self-assembly structure such as the large dissimilarity of the conformationally distinct two blocks and the π–π interaction between rigid conjugated blocks.[42,43] The nanofiber morphology has been seen in other rod–coil block copolymer systems[44,45] and is typically driven by the packing of the conjugated block.[46] However, previous studies on amphiphilic molecules containing different types of conjugated oligomers (*e.g.*, tetra-*p*-phenylene, isocyano(L-alanylaminoethyl)-thiophene) have shown that various types of self-assembly structures such as spherical micelles and vesicles can be formed in addition to one-dimensional rods and wires by varying the relative rod to coil lengths.[47,48] On the contrary, the study presented herein on PHT-*b*-PEG shows that the nanofiber structure is prevalent for a broad range of f_{PHT} (f_{PHT} = 0.41, 0.61, and 0.82) due to the strong

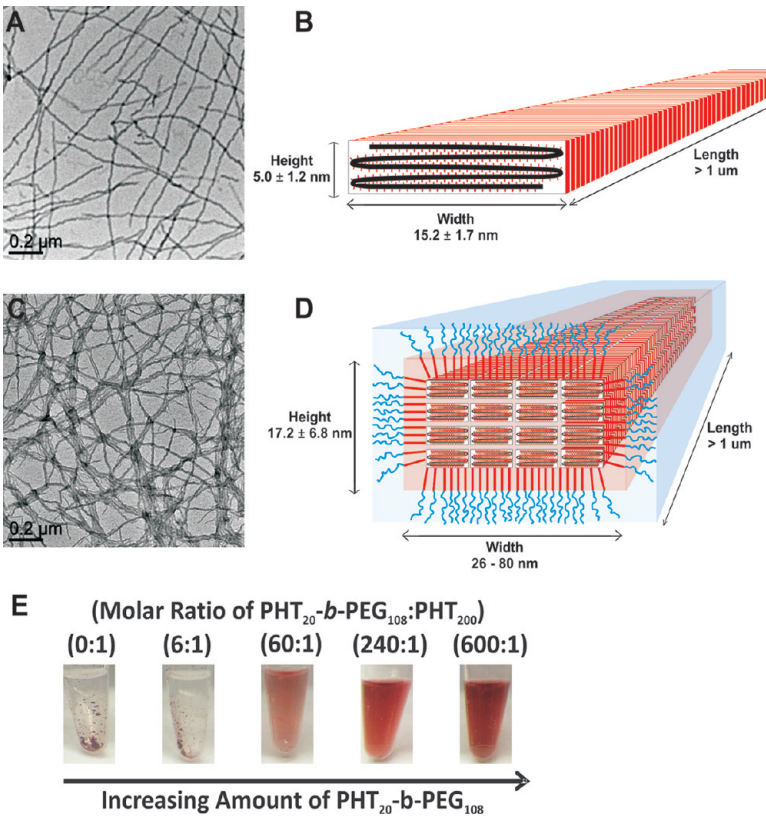

Figure 3. (A) TEM image of PHT_{200} nanofibers in anisole. (B) Pictorial description of PHT_{200} nanofibers. (C) TEM image of PHT_{200} nanofiber bundles encapsulated in PHT_{20}-*b*-PEG_{108} in methanol. (D) Pictorial description of superstructure (fiber bundles) formed in methanol. (E) Pictures of PHT_{200} nanofibers in 99% methanol/1% anisole with increasing amounts of PHT_{20}-*b*-PEG_{108}.

tendency of PHT to form well-packed quasi-one-dimensional crystals.

The length of the nanofibers was found to gradually increase with decreasing PEG block lengths (Figure 2A–C). At f_{PHT} of 0.41 and 0.60, the lengths of nanofibers were ~40–100 nm (Figure 4A) and ~150–400 nm (Figure 4B), respectively. At the largest f_{PHT} of 0.82, longer nanofibers with a length of >1000 nm were commonly observed (Figure 4C). The increase of the aggregation number with the increase of f_{PHT} was also confirmed by dynamic light scattering (DLS) analysis (Figure S10). Similar behavior has been previously found in amphiphilic conjugated oligomers of pyrene-*b*-tetra-*p*-phenylene-*b*-PEG[49] and oligo(*p*-phenylenevinylene)-*b*-PEG[50] and can be explained by the reduction of the stretching energy of long PEG chains through adopting shorter fibers. On the other hand, the widths of the nanofibers (Figure S11) and the UV–vis absorption and PL characteristics (Figure S12) were not significantly affected by the length of PEG. This result indicates that the packing of PHT is the determining factor for the solution-phase morphology for a wide range of f_{PHT}, and that the packing structure of PHT in the fiber, which is closely related to transport properties, does not significantly change with the length of the PEG block and the length of nanofibers. Note that the formation of uniform assemblies of PHT-*b*-PEG in this study is in part a result of the low polydispersity of PHT-*b*-PEG synthesized by click chemistry. When the assemblies were formed from polymer mixtures, resulting nanofibers had a broad range of lengths as expected (Figure S13).

Self-Assembly of PHT Nanofibers into Bundled and Branched Superstructures. We further utilized the self-assembly of PHT_{20}-*b*-PEG_{108} to organize and solubilize preformed nanofibers of PHT homopolymers. High molecular weight homopolymers of PHT tend to crystallize into long fibers in marginal solvents.[51−53] Typically, high aspect ratio nanofibers of PHT were prepared by slowly cooling a hot (70 °C) anisole solution of commercial PHT_{200} (1 mg/mL), following a modified literature procedure[34] (Figure 3A,B). The dimensions of the PHT_{200} nanofibers were similar to those reported in the literature;[54] the PHT_{200} nanofibers had the average width of 15.2 ± 1.7 nm and a very high aspect ratio with a length of 1–10 μm measured by TEM and an average height of 5.0 ± 1.2 nm measured by AFM. The preformed PHT_{200} nanofibers were organized into fiber bundles or branched fibers by the self-assembly with PHT-*b*-PEG. In typical experiments, PHT_{20}-*b*-PEG_{108} was added to PHT_{200} nanofibers in anisole, followed by the addition of either water or methanol. After mixing overnight, the residual anisole was dissipated under a low nitrogen flow.

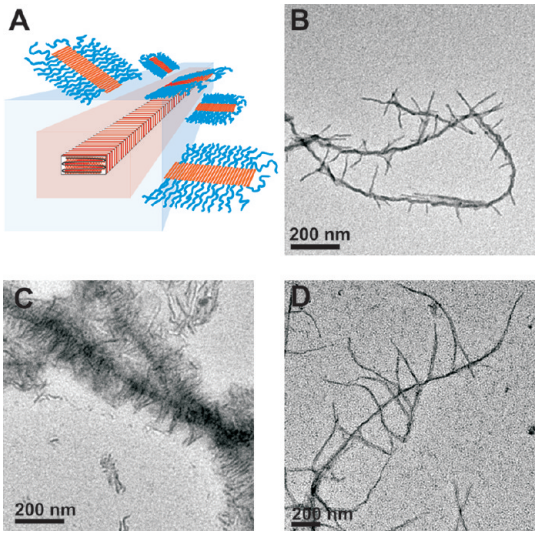

Figure 4. (A) Pictorial description of the branched superstructure composed of PHT_{200} nanofibers and PHT_{20}-*b*-PEG_{108}. TEM images of (B) a branched structure composed of PHT_{200} nanofibers decorated with low density PHT_{20}-*b*-PEG_{108} nanofibers formed at a molar ratio of 60:1 (PHT_{20}-*b*-PEG_{108}/PHT_{200}), (C) a high density branched structure composed of PHT_{200} nanofibers decorated with PHT_{20}-*b*-PEG_{108} nanofibers at a molar ratio of 480:1 (PHT_{20}-*b*-PEG_{108}/PHT_{200}), and (D) a branched structure composed of PHT_{200} nanofibers decorated with longer PHT_{20}-*b*-PEG_{48} nanofibers formed at a molar ratio of 250:1 (PHT_{20}-*b*-PEG_{48}/PHT_{200}).

When methanol was used to drive the self-assembly, PHT nanofibers were encapsulated in PHT_{20}-*b*-PEG_{108} as fiber bundles (Figure 3C,D). The width of the bundles was about 26−80 nm, corresponding to 2−6 fibers, and the length of the bundles was typically 1−10 μm, as determined by TEM. A critical amount of PHT_{20}-*b*-PEG_{108} was necessary to encapsulate and transfer PHT_{200} nanofibers into polar solvents. At low PHT_{20}-*b*-PEG_{108} concentrations, PHT_{200} nanofibers precipitated out of solution upon the addition of methanol (Figure 3E). When sufficient amounts of PHT_{20}-*b*-PEG_{108} were added, PHT nanofibers were encapsulated by PHT_{20}-*b*-PEG_{108} and stayed well-dispersed in methanol. Adding an excess amount of PHT_{20}-*b*-PEG_{108} did not notably change the structure of the encapsulated PHT_{200} nanofibers, but instead resulted in isolated PHT_{20}-*b*-PEG_{108} nanofibers (Figure 1C) coexisting with bundled PHT_{200} nanofibers.

A distinct type of superstructure of branched fibers was formed when water was used to induce the self-assembly instead of methanol (Figure 4A). The resulting superstructure was composed of PHT_{20}-*b*-PEG_{108} fibers perpendicularly grown off of PHT_{200} nanofibers. This branched structure is reminiscent of the crystallization of PHT homopolymers on PHT nanofibers[55,56] and carbon nanotubes.[57] The width of the PHT_{20}-*b*-PEG_{108} nanofiber branches was 7.9 $\pm$ 1.2 nm, which is similar to the dimension of isolated PHT_{20}-*b*-PEG_{108} nanofibers shown in Figure 1C. The origin of the lateral growth of PHT_{20}-*b*-PEG_{108} nanofibers is believed to be associated with the immiscibility of water and anisole. Upon the addition of water, PHT_{20}-*b*-PEG_{108} nanofibers are likely to be formed in water while PHT_{200} nanofibers remain in anisole. When the anisole is dissipated under nitrogen flow, the high energy tip of the preformed PHT_{20}-*b*-PEG_{108} fibers stack onto PHT_{200} nanofibers, forming the distinctive supramolecular structure and bringing PHT_{200} nanofibers into water. As in the methanol case, a critical amount of PHT_{20}-*b*-PEG_{108} was needed to disperse the PHT_{200} nanofibers in water. The length of nanofiber branches was quite uniform, and the density of nanofiber branches can be controlled by changing the concentration of PHT_{20}-*b*-PEG_{108}, as shown in Figure 4B,C. As shown above, the length of PHT-*b*-PEG fibers can be controlled by varying the length of PEG (Figure 2). This behavior was applied to control the lengths of PHT-*b*-PEG nanofibers in the branched superstructure. When PHT_{20}-*b*-PEG_{48} is used instead of PHT_{20}-*b*-PEG_{108}, a similar superstructure was obtained with longer branches (Figure 4D).

CONCLUSIONS

A series of different length PHT_m-*b*-PEG_n (m = 20, n = 16, 48, 108) was synthesized in high yields (>70%) by copper-catalyzed click chemistry. The molecular weight and relative block lengths of the synthesized polymers were determined by thoroughly characterizing each block prior to coupling, which allowed for a systematic study of the block length effect on the self-assembly structure. In selective solvents such as water and methanol, PHT_m-*b*-PEG_n self-assembled into interdigitated one-dimensional assemblies (nanofibers). The self-assembly of PHT_m-*b*-PEG_n accompanied an efficient PL quenching and red shift of absorption spectra, indicating a tight packing of PHT in the assembly structure. The length of nanofibers was increased with decreasing PEG lengths due to the reduced stretching energy, and a large f_{PHT} of 0.82 led to the formation of micrometer-long nanofibers. The wire-like morphology was maintained for a wide range of relative polymer lengths with weight factions of PHT (f_{PHT}) varying from 0.41 to 0.82, indicating that the packing of PHT is the main factor that controls the self-assembly structure. In addition, the width and optical properties of PHT_m-*b*-PEG_n nanofibers did not change significantly with the relative PEG block length, which shows that the lengths of nanofibers can be controlled without changing the packing structure and properties (optical, transport) of PHT in the nanofibers. The PHT_m-*b*-PEG_n nanofibers were further used as building blocks to form hierarchical assemblies of nanofibers. The self-assembly of PHT_m-*b*-PEG_n and preformed nanofibers of high molecular weight PHT (PHT_{200}) in methanol led to the formation of bundled nanofibers encapsulated in PHT_m-*b*-PEG_n. In addition, unique superstructures of branched nanofibers were

formed when water was used for the self-assembly instead of methanol. The density and the length of nanofiber branches in the superstructure could be controlled by varying the concentration and the length of PEG, respectively. The controlled self-assembly and encapsulation strategy presented here provides a new toolbox toward the fabrication of novel organic semiconducting nanostructures.

METHODS

Materials and Instrumentation. Methanol, hexane, and chloroform were purchased from Fisher Scientific. Regioregular (>95% HT) PHT with a number average molecular weight of 33 405 g mol^{-1} was purchased from Sigma Aldrich. All other reagents were also purchased from Sigma Aldrich. THF was freshly distilled prior to use from sodium/benzophenone under nitrogen, and all other reagents were used without further purification. All reactions were performed in oven-dried glassware under prepurified nitrogen.

Electronic absorption spectra were acquired on an Agilent 8453 spectrophotometer. Emission spectra were acquired on a Spex Fluorolog 3 utilizing a R928 PMT detector. Proton NMR spectra were obtained on a Bruker-DMX500 interfaced to an Aspect 3000 computer in $CDCl_3$ at ambient temperature. IR spectra were obtained on a Perkin-Elmer system 2000 FTIR spectrometer. TEM was performed on a JEOL 1400 electron microscope operating at 120 kV accelerating voltage. GPC measurements were carried out at room temperature at a flow rate of 1.0 mL/min on a Shimadzu LC-10AT liquid chromatography system equipped with a series of two PLgel 10 μm 10E6A columns, an SPD-10AVvp absorbance UV/vis detector, and a refractive index detector (RID-10A) calibrated against linear polystyrene standards in THF. DLS measurements were taken on a Malvern Zetasizer Nano Series. Matrix-assisted laser desorption ionization time-of-flight mass spectrometry (MALDI-TOF/TOF MS) spectra were obtained on a Bruker Flex Series MALDI-TOF/TOF MS. Spectra were recorded in the positive-ion reflectron mode with an accelerating voltage of 20 kV. The MALDI samples were prepared by mixing a THF solution of PHT (10 mg/mL) and a THF solution of 2,2′:5,2″-terthiophene matrix solution (0.25 M). For PEG samples, a THF solution of 4′-hydroxyazobenzene-2-carboxylic acid (HABA) (0.25 M) was used as a matrix and was mixed with a THF solution of PEG (10 mg/mL). The MALDI sample was prepared by depositing 1 μL of a (1 matrix/1 sample) solution on the stainless steel sample target and then letting the sample air-dry.

Synthesis of Ethynyl-PHT. The monoethynyl-terminated poly(3-hexylthiophene) (ethynyl-PHT) was synthesized following a previously reported method (Scheme 1).[23,24] In a typical experiment, 2,5-dibromohexylthiophene (1.8 g, 5.6 mmol) and 10 mL of freshly distilled THF were added to a 100 mL round-bottom flask and the system was purged with nitrogen. A 1.0 M solution of *tert*-butylmagnesium chloride in THF (5.6 mL, 5.6 mmol) was then added, and the mixture was stirred for 3 h at room temperature under nitrogen. During this time, the solution changed from a yellow color to a green color. The mixture was then diluted with 30 mL of THF followed by addition of Ni(dppp)Cl_2 (70 mg, 0.1 mmol). The reaction proceeded under nitrogen flow for an additional 20 min, and then a 0.5 M solution of ethynyl magnesium bromide in THF (2.8 mL, 1.4 mmol) was added and reacted for an additional 20 min. At this time, the reaction was quenched by adding methanol and then the product was purified by subsequent Soxhlet extractions with methanol and hexanes. The final product was then collected by a final Soxhlet extraction with chloroform. The ethynyl-PHT solid product (purple solid) was dried to a constant weight under vacuum (372 mg, 0.12 mmol) and then stored under inert atmosphere. ^{1}H NMR (500 MHz, $CDCl_3$): δ_H 0.89 (t, 3H), 1.32−1.42 (m, 6H), 1.68 (t, 2H), 2.78 (t, 2H), 3.51 (s), 6.98 (s, 1H). GPC: M_n = 6562, PDI = 1.17. MALDI-MS: m/z = 3428.87 [M+] (calcd 3428, degree of polymerization (DP) of 20, ethynyl/Br end groups), PDI = 1.16.

Synthesis of Azide-PEG. The monoazide-terminated poly(ethylene glycol) (azide-PEG) was synthesized following a modified literature procedure.[25,26] Azide-PEG was synthesized by mesylation of the hydroxyl terminus of commercial methoxy-PEG followed by sodium azide substitution. Typically, a solution of methoxy-PEG (4.4 g, 0.92 mmol), triethylamine (0.51 mL, 3.7 mmol), and 50 mL of freshly distilled THF was added to a three-neck round-bottom flask, and the system was purged with nitrogen. Methanesulfonyl chloride (0.32 mL, 4.1 mmol) was then added to the flask, and the solution was stirred at room temperature for 10 h. The reaction product was then dried down using rotary evaporation, redissolved into minimal amount of deionized water (~1−2 mL), and then extracted into DCM (150 mL × 2). After drying the organic product layer with sodium sulfate, the product was filtered, concentrated, and then precipitated from minimal DCM into cold diethyl ether. The off-white/yellow precipitate was then filtered, washed with cold diethyl ether, and then dried under vacuum to a constant weight (3.9 g, 88%). The mesylated PEG (3.9 g, 0.81 mmol) was added to a round-bottom flask with 50 mL of DMF and a reflux condenser. Sodium azide (4.3 g, 65 mmol) was then added to the flask, and the solution was heated at 60 °C for 24 h. The reaction product was then dried down using rotary evaporation. The product was then redissolved into DCM, and the excess sodium azide was removed by filtration. The product in DCM was further cleaned by extraction with brine solution (100 mL × 4). After drying the organic layer with sodium sulfate, the product was filtered, concentrated, and then precipitated from minimal DCM into cold diethyl ether. The azide-PEG product (white solid) was then filtered, washed with cold diethyl ether, and then dried under vacuum to a constant weight (2.2 g, 57%). Characterization of azide-PEG_{108}. IR (KBr, cm^{-1}): 2101 (azide), 529, 842, 963, 1108, 1237, 1282, 1343, 1468. MALDI-MS: m/z = 4896.35 [M+] (calcd 4896, DP of 108, N_3/CH_3 end groups), PDI = 1.21. Characterization of azide-PEG_{48}. IR (KBr, cm^{-1}): 2100 (azide), 529, 842, 963, 1108, 1237, 1282, 1343, 1468. MALDI-MS: m/z = 2167.1 [M+] (calcd 2169.02, DP of 48, N_3/CH_3 end groups), PDI = 1.18. Characterization of azide-PEG_{16}. IR (KBr, cm^{-1}): 2100 (azide), 529, 842, 963, 1108, 1237, 1282, 1343, 1468. MALDI-MS: m/z = 759.5 [M+] (calcd 761.02, DP of 16, N_3/CH_3 end groups), PDI = 1.22.

Synthesis of Poly(3-hexylthiophene)-*block*-Poly(ethylene glycol). PHT-*b*-PEG was synthesized by the copper(I)-catalyzed click reaction between azide-PEG and ethynyl-PHT (Scheme 1). Typically, ethynyl-PHT (100 mg, 0.0266 mmol), azide-terminated PEG (257 mg, 0.0532 mmol), and 10 mL of freshly distilled THF were added to a 25 mL Schlenk flask. A solution of 1,8-diazabicyclo-[5.4.0]undec-7-ene (DBU) (152.2 mg, 1.0 mmol) and copper(I) iodide (1.9 mg, 0.010 mmol) was then degassed and then introduced into the Schlenk flask. The mixture was then degassed with three freeze−pump−thaw cycles and subsequently refilled with nitrogen. The solution reacted at 40 °C for 4 days. The excess copper salt and excess PEG homopolymer was removed by passing the product through a neutral alumina column. After the removal of THF by rotary evaporation, the product was precipitated into methanol and then filtered to remove any excess PHT homopolymer. The final product was washed with hexanes and then dried under vacuum and collected as a purple solid (229 mg, 92% yield). ^{1}H NMR (500 MHz, $CDCl_3$): δ_H 0.89 (t, 3H), 1.32−1.42 (m, 6H), 1.68 (t, 2H), 2.78 (t, 2H), 3.61 (s), 6.95 (s).

Preparation of PHT_{200} Nanofibers. The commercial PHT was purified by sequential Soxhlet extractions with hexanes, DCM, and THF to remove lower molecular weight fractions (<22 000 g/mol). The purified higher molecular weight product was then collected by a final Soxhlet extraction with chloroform and used for subsequent experiments. In order to prepare the PHT_{200} nanofibers, regioregular (>95% HT) poly(3-hexylthiophene) with a number average molecular weight of 33 405 g mol^{-1}

(PHT_{200}) was dissolved in anisole at a concentration of 1 mg/mL. This solution was heated to 70 °C in a hot water bath for 1 h, yielding a clear orange solution. The hot solution was then cooled to room temperature by placing in a drawer overnight to allow for complete crystallization as evidenced by the color change of the solution from orange to purple. The aged solution was then centrifuged at 5000 rpm for 30 min (×2) to isolate PHT_{200} crystallized nanofibers.

Preparation of PHT_{200} Nanofibers Encapsulated in PHT_{20}-*b*-PEG_{108}. In a typical encapsulation experiment with a molar ratio of PHT_{20}-*b*-PEG_{108}/PHT_{200} of 173:1, 800 μL of a 5.12×10^{-5} M stock solution of PHT_{20}-*b*-PEG_{108} in chloroform (concentration determined from UV−vis with an extinction coefficient of 4.3×10^4 M^{-1} cm^{-1}) was first dried down under nitrogen. Then, a 10 μL aliquot of a 2.37×10^{-5} M stock solution of PHT_{200} nanofibers in anisole (concentration determined from UV−vis with an extinction coefficient of 1×10^6 M^{-1} cm^{-1}) was added to the dried block copolymer. After 20 min of mixing, either 1000 μL of water or 1000 μL of methanol was added to the solution. The assemblies were mixed for 15 h at 200 rpm on a shaker, and then a low flow of nitrogen was used to dissipate anisole in the solution. Harsher mixing procedures such as vortexing or sonication were avoided because they caused significant entangling of PHT superstructures. After dissipation of any residual anisole, either methanol or water was added to the solution until a final volume of 1 mL of solution was reached. In some cases, the superstructures were purified and concentrated by the centrifugation at 2000 rpm for 45 min.

Conflict of Interest: The authors declare no competing financial interest.

Acknowledgment. This material is based upon work supported in part by the U.S. Army Research Laboratory and the U.S. Army Research Office under Contract/Grant No. W911NF-09-1-0146. A.C.K. acknowledges the support from the Nano/Bio Interface Center through the National Science Foundation IGERT DGE02-21664.

Supporting Information Available: Detailed synthesis and characterization of PHT-*b*-PEG, self-assembly and optical properties of PHT-*b*-PEG in selective solvents, detailed information on the effect of polymer length dependence, and more detailed information on the self-assembly and optical properties of PHT nanofiber superstructures. This material is available free of charge *via* the Internet at http://pubs.acs.org.

REFERENCES AND NOTES

1. Schenning, A.; Meijer, E. W. Supramolecular Electronics; Nanowires from Self-Assembled π-Conjugated Systems. *Chem. Commun.* **2005**, 3245–3258.
2. He, M.; Han, W.; Ge, J.; Yang, Y.; Qiu, F.; Lin, Z. All-Conjugated Poly(3-alkylthiophene) Diblock Copolymer-Based Bulk Heterojunction Solar Cells with Controlled Molecular Organization and Nanoscale Morphology. *Energy Environ. Sci.* **2011**, *4*, 2894–2902.
3. He, M.; Qiu, F.; Lin, Z. Conjugated Rod−Coil and Rod−Rod Block Copolymers for Photovoltaic Applications. *J. Mater. Chem.* **2011**, *21*, 17039–17048.
4. Moliton, A.; Hiorns, R. C. Review of Electronic and Optical Properties of Semiconducting π-Conjugated Polymers: Applications in Optoelectronics. *Polym. Int.* **2004**, *53*, 1397–1412.
5. Pal, T.; Arif, M.; Khondaker, S. I. High Performance Organic Phototransistor Based on Regioregular Poly(3-hexylthiophene). *Nanotechnology* **2010**, *21*, 1–5.
6. Wu, Z.; Petzold, A.; Henze, T.; Thurn-Albrecht, T.; Lohwasser, R. H.; Sommer, M.; Thelakkat, M. Temperature and Molecular Weight Dependent Hierarchical Equilibrium Structures in Semiconducting Poly(3-hexylthiophene). *Macromolecules* **2010**, *43*, 4646–4653.
7. Schwartz, B. J. Conjugated Polymers as Molecular Materials: How Chain Conformation and Film Morphology Influence Energy Transfer and Interchain Interactions. *Annu. Rev. Phys. Chem.* **2003**, *54*, 141–172.
8. Yang, H.; Shin, T. J.; Bao, Z.; Ryu, C. Y. Structural Transitions of Nanocrystalline Domains in Regioregular Poly(3-hexyl thiophene) Thin Films. *J. Polym. Sci., Part B: Polym. Phys.* **2007**, *45*, 1303–1312.
9. Lee, S. S.; Kim, C. S.; Gomez, E. D.; Purushothaman, B.; Toney, M. F.; Wang, C.; Hexemer, A.; Anthony, J. E.; Loo, Y.-L. Controlling Nucleation and Crystallization in Solution-Processed Organic Semiconductors for Thin-Film Transistors. *Adv. Mater.* **2009**, *21*, 3605–3609.
10. Gao, Y.; Martin, T. P.; Niles, E. T.; Wise, A. J.; Thomas, A. K.; Grey, J. K. Understanding Morphology-Dependent Polymer Aggregation Properties and Photocurrent Generation in Polythiophene/Fullerene Solar Cells of Variable Compositions. *J. Phys. Chem. C* **2010**, *114*, 15121–15128.
11. Olsen, B. D.; Li, X.; Wang, J.; Segalman, R. A. Thin Film Structure of Symmetric Rod−Coil Block Copolymers. *Macromolecules* **2007**, *40*, 3287–3295.
12. Hamley, I. W. Ordering in Thin Films of Block Copolymers: Fundamentals to Potential Applications. *Prog. Polym. Sci.* **2009**, *34*, 1161–1210.
13. Hlaing, H.; Lu, X.; Hofmann, T.; Yager, K. G.; Black, C. T.; Ocko, B. M. Nanoimprint-Induced Molecular Orientation in Semiconducting Polymer Nanostructures. *ACS Nano* **2011**, *5*, 7532–7538.
14. Ho, V.; Boudouris, B. W.; McCulloch, B. L.; Shuttle, C. G.; Burkhardt, M.; Chabinyc, M. L.; Segalman, R. A. Poly(3-alkylthiophene) Diblock Copolymers with Ordered Microstructures and Continuous Semiconducting Pathways. *J. Am. Chem. Soc.* **2011**, *133*, 9270–9273.
15. Dai, C.-A.; Yen, W.-C.; Lee, Y.-H.; Ho, C.-C.; Su, W.-F. Facile Synthesis of Well-Defined Block Copolymers Containing Regioregular Poly(3-hexyl thiophene) *via* Anionic Macroinitiation Method and Their Self-Assembly Behavior. *J. Am. Chem. Soc.* **2007**, *129*, 11036–11038.
16. Iovu, M. C.; Jeffries-El, M.; Zhang, R.; Kowalewski, T.; McCullough, R. D. Conducting Block Copolymer Nanowires Containing Regioregular Poly(3-hexylthiophene) and Polystyrene. *J. Macromol. Sci., Part A: Pure Appl. Chem.* **2006**, *43*, 1991–2000.
17. Tu, G. L.; Li, H. B.; Forster, M.; Heiderhoff, R.; Balk, L. J.; Sigel, R.; Scherf, U. Amphiphilic Conjugated Block Copolymers: Synthesis and Solvent-Selective Photoluminescence Quenching. *Small* **2007**, *3*, 1001–1006.
18. Park, S. J.; Kang, S. G.; Fryd, M.; Saven, J. G.; Park, S. J. Highly Tunable Photoluminescent Properties of Amphiphilic Conjugated Block Copolymers. *J. Am. Chem. Soc.* **2010**, *132*, 9931–9933.
19. Lee, E.; Hammer, B.; Kim, J.-K.; Page, Z.; Emrick, T.; Hayward, R. C. Hierarchical Helical Assembly of Conjugated Poly(3-hexylthiophene)-*Block*-Poly(3-triethylene glycol thiophene) Diblock Copolymers. *J. Am. Chem. Soc.* **2011**, *133*, 10390–10393.
20. Gaedt, T.; Ieong, N. S.; Cambridge, G.; Winnik, M. A.; Manners, I. Complex and Hierarchical Micelle Architectures from Diblock Copolymers Using Living, Crystallization-Driven Polymerizations. *Nat. Mater.* **2009**, *8*, 144–150.
21. Patra, S. K.; Ahmed, R.; Whittell, G. R.; Lunn, D. J.; Dunphy, E. L.; Winnik, M. A.; Manners, I. Cylindrical Micelles of Controlled Length with a π-Conjugated Polythiophene Core *via* Crystallization-Driven Self-Assembly. *J. Am. Chem. Soc.* **2011**, *133*, 8842–8845.
22. Bock, V. D.; Hiemstra, H.; van Maarseveen, J. H. Cu-I-Catalyzed Alkyne-Azide "Click" Cycloadditions from a Mechanistic and Synthetic Perspective. *Eur. J. Org. Chem.* **2005**, 51–68.
23. Jeffries-El, M.; Sauve, G.; McCullough, R. D. Facile Synthesis of End-Functionalized Regioregular Poly(3-alkylthiophene)s *via* Modified Grignard Metathesis Reaction. *Macromolecules* **2005**, *38*, 10346–10352.
24. Iovu, M. C.; Jeffries-El, M.; Sheina, E. E.; Cooper, J. R.; McCullough, R. D. Regioregular Poly(3-alkylthiophene) Conducting Block Copolymers. *Polymer* **2005**, *46*, 8582–8586.
25. Szwarc, M.; Levy, M.; Milkovich, R. Polymerization Initiated by Electron Transfer to Monomer—A New Method of

Formation of Block Polymers. *J. Am. Chem. Soc.* **1956**, *78*, 2656–2657.
26. Hiki, S.; Kataoka, K. A Facile Synthesis of Azido-Terminated Heterobifunctional Poly(ethylene glycol)s for "Click" Conjugation. *Bioconjugate Chem.* **2007**, *18*, 2191–2196.
27. Li, Z.; Ono, R. J.; Wu, Z.-Q.; Bielawski, C. W. Synthesis and Self-Assembly of Poly(3-hexylthiophene)-*Block*-Poly(acrylic acid). *Chem. Commun.* **2011**, *47*, 197–199.
28. Urien, M.; Erothu, H.; Cloutet, E.; Hiorns, R. C.; Vignau, L.; Cramail, H. Poly(3-hexylthiophene) Based Block Copolymers Prepared by "Click" Chemistry. *Macromolecules* **2008**, *41*, 7033–7040.
29. Wu, Z.-Q.; Ono, R. J.; Chen, Z.; Bielawski, C. W. Synthesis of Poly(3-alkylthiophene)-*Block*-Poly(arylisocyanide): Two Sequential, Mechanistically Distinct Polymerizations Using a Single Catalyst. *J. Am. Chem. Soc.* **2010**, *132*, 14000–14001.
30. Alemseghed, M. G.; Servello, J.; Hundt, N.; Sista, P.; Biewer, M. C.; Stefan, M. C. Amphiphilic Block Copolymers Containing Regioregular Poly(3-hexylthiophene) and Poly(2-ethyl-2-oxazoline). *Macromol. Chem. Phys.* **2010**, *211*, 1291–1297.
31. Braunecker, W. A.; Matyjaszewski, K. Controlled/Living Radical Polymerization: Features, Developments, and Perspectives. *Prog. Polym. Sci.* **2007**, *32*, 93–146.
32. Holdcroft, S. Determination of Molecular-Weights and Mark-Houwink Constants for Soluble Electronically Conducting Polymers. *J. Polym. Sci., Part B: Polym. Phys.* **1991**, *29*, 1585–1588.
33. McCullough, R. D. The Chemistry of Conducting Polythiophenes. *Adv. Mater.* **1998**, *10*, 93–116.
34. Samitsu, S.; Shimomura, T.; Heike, S.; Hashizume, T.; Ito, K. Effective Production of Poly(3-alkylthiophene) Nanofibers by Means of Whisker Method Using Anisole Solvent: Structural, Optical, and Electrical Properties. *Macromolecules* **2008**, *41*, 8000–8010.
35. Ihn, K. J.; Moulton, J.; Smith, P. Whiskers of Poly(3-alkylthiophene)s. *J. Polym. Sci., Part B: Polym. Phys.* **1993**, *31*, 735–742.
36. Sun, S.; Salim, T.; Wong, L. H.; Foo, Y. L.; Boey, F.; Lam, Y. M. A New Insight into Controlling Poly(3-hexylthiophene) Nanofiber Growth through a Mixed-Solvent Approach for Organic Photovoltaics Applications. *J. Mater. Chem.* **2011**, *21*, 377–386.
37. Brinkmann, M.; Rannou, P. Molecular Weight Dependence of Chain Packing and Semicrystalline Structure in Oriented Films of Regioregular Poly(3-hexylthiophene) Revealed by High-Resolution Transmission Electron Microscopy. *Macromolecules* **2009**, *42*, 1125–1130.
38. Choi, S. Y.; Lee, J. U.; Lee, J. W.; Lee, S.; Song, Y. J.; Jo, W. H.; Kim, S. H. Highly Ordered Poly(3-hexylthiophene) Rod Polymers *via* Block Copolymer Self-Assembly. *Macromolecules* **2011**, *44*, 1771–1774.
39. Iovu, M. C.; Zhang, R.; Cooper, J. R.; Smilgies, D. M.; Javier, A. E.; Sheina, E. E.; Kowalewski, T.; McCullough, R. D. Conducting Block Copolymers of Regioregular Poly(3-hexylthiophene) and Poly(methacrylates): Electronic Materials with Variable Conductivities and Degrees of Interfibrillar Order. *Macromol. Rapid Commun.* **2007**, *28*, 1816–1824.
40. Tao, Y.; McCulloch, B.; Kim, S.; Segalman, R. A. The Relationship between Morphology and Performance of Donor–Acceptor Rod–Coil Block Copolymer Solar Cells. *Soft Matter* **2009**, *5*, 4219–4230.
41. Zhang, L. F.; Eisenberg, A. Formation of Crew-Cut Aggregates of Various Morphologies from Amphiphilic Block Copolymers in Solution. *Polym. Adv. Technol.* **1998**, *9*, 677–699.
42. Chou, S.-H.; Tsao, H.-K.; Sheng, Y.-J. Structural Aggregates of Rod–Coil Copolymer Solutions. *J. Chem. Phys.* **2011**, *134*, 034904.
43. Olsen, B. D.; Segalman, R. A. Self-Assembly of Rod–Coil Block Copolymers. *Mater. Sci. Eng., R* **2008**, *62*, 37–66.
44. Wang, H. B.; Wang, H. H.; Urban, V. S.; Littrell, K. C.; Thiyagarajan, P.; Yu, L. P. Syntheses of Amphiphilic Diblock Copolymers Containing a Conjugated Block and Their Self-Assembling Properties. *J. Am. Chem. Soc.* **2000**, *122*, 6855–6861.
45. de Cuendias, A.; Ibarboure, E.; Lecommandoux, S.; Cloutet, E.; Cramail, H. Synthesis and Self-Assembly in Water of Coil–Rod–Coil Amphiphilic Block Copolymers with Central π-Conjugated Sequence. *J. Polym. Sci., Part A: Polym. Chem.* **2008**, *46*, 4602–4616.
46. Lin, J.; Lin, S.; Zhang, L.; Nose, T. Microphase Separation of Rod–Coil Diblock Copolymer in Solution. *J. Chem. Phys.* **2009**, 130.
47. Ryu, J.-H.; Hong, D.-J.; Lee, M. Aqueous Self-Assembly of Aromatic Rod Building Blocks. *Chem. Commun.* **2008**, 1043–1054.
48. Vriezema, D. M.; Hoogboom, J.; Velonia, K.; Takazawa, K.; Christianen, P. C. M.; Maan, J. C.; Rowan, A. E.; Nolte, R. J. M. Vesicles and Polymerized Vesicles from Thiophene-Containing Rod–Coil Block Copolymers. *Angew. Chem.* **2003**, *42*, 772–776.
49. Han, K.-H.; Lee, E.; Kim, J. S.; Cho, B.-K. An Extraordinary Cylinder-to-Cylinder Transition in the Aqueous Assemblies of Fluorescently Labeled Rod–Coil Amphiphiles. *J. Am. Chem. Soc.* **2008**, *130*, 13858–13859.
50. Mori, T.; Watanabe, T.; Minagawa, K.; Tanaka, M. Self-Assembly of Oligo(*p*-phenylenevinylene)-*Block*-Poly(ethylene oxide) in Polar Media and Solubilization of an Oligo(*p*-Phenylenevinylene) Homooligomer Inside the Assembly. *J. Polym. Sci., Part A: Polym. Chem.* **2005**, *43*, 1569–1578.
51. Berson, S.; De Bettignies, R.; Bailly, S.; Guillerez, S. Poly(3-hexylthiophene) Fibers for Photovoltaic Applications. *Adv. Funct. Mater.* **2007**, *17*, 1377–1384.
52. Oosterbaan, W. D.; Vrindts, V.; Berson, S.; Guillerez, S.; Douhéret, O.; Ruttens, B.; D'Haen, J.; Adriaensens, P.; Manca, J.; Lutsen, L.; *et al.* Efficient Formation, Isolation and Characterization of Poly(3-alkylthiophene) Nanofibres: Probing Order as a Function of Side-Chain Length. *J. Mater. Chem.* **2009**, *19*, 5424.
53. Hammer, B. A. G.; Bokel, F. A.; Hayward, R. C.; Emrick, T. Cross-Linked Conjugated Polymer Fibrils: Robust Nanowires from Functional Polythiophene Diblock Copolymers. *Chem. Mater.* **2011**, *23*, 4250–4256.
54. Liu, J.; Arif, M.; Zou, J.; Khondaker, S. I.; Zhai, L. Controlling Poly(3-hexylthiophene) Crystal Dimension: Nanowhiskers and Nanoribbons. *Macromolecules* **2009**, *42*, 9390–9393.
55. Brinkmann, M.; Chandezon, F.; Pansu, R. B.; Julien-Rabant, C. Epitaxial Growth of Highly Oriented Fibers of Semiconducting Polymers with a Shish-Kebab-like Superstructure. *Adv. Funct. Mater.* **2009**, *19*, 2759–2766.
56. Yan, H.; Yan, Y.; Yu, Z.; Wei, Z. Self-Assembling Branched and Hyperbranched Nanostructures of Poly(3-hexylthiophene) by a Solution Process. *J. Phys. Chem. C* **2011**, *115*, 3257–3262.
57. Liu, J.; Zou, J.; Zhai, L. Bottom-Up Assembly of Poly(3-hexylthiophene) on Carbon Nanotubes: 2D Building Blocks for Nanoscale Circuits. *Macromol. Rapid Commun.* **2009**, *30*, 1387–1391.